CIVIL ENGINEERING JOURNAL

Article no. 17

THE CIVIL ENGINEERING JOURNAL 2-2025

EXPERIMENTAL VERIFICATION OF THE INFLUENCE OF THE QUALITY OF INPUT IMAGES ON THE PROCESSING OF THE PHOTOGRAMMETRIC MODEL

Alice Adamcová

Czech Technical University in Prague, Faculty of Civil Engineering, Department of Special Geodesy, Thákurova 7, 166 29, Praha 6, Czech Republic; alice.adamcova@fsv.cvut.cz

Received: 09.01.2025
Received in revised form: 30.04.2025
Accepted: 24.07.2025

ABSTRACT

Photogrammetric acquisition and subsequent data processing have become increasingly common in recent years. However, this method of documentation is affected by many circumstances that can negatively influence the results. This paper is devoted to the experimental determination of the influence of the quality of input images on the processing of a photogrammetric model, because the quality of input images is essential for the accuracy of the final product and can be influenced by various factors. The effect of different image quality on the ability of software to align these images and on the accuracy of this alignment and subsequent processing was tested practically in this case. Three specific interior surfaces and three specific exterior surfaces were used for the experiment, each of which was photographed in four series - one series was taken with high quality images, while the remaining three were specifically degraded in quality. Three photogrammetric software, Agisoft Metashape Professional, iTwin Capture Modeler and Pix4Dmapper, were selected for processing. In all software, all acquired series were processed and the ability to perform image orientation and the subsequent quality of this orientation was mainly monitored, where reprojection error was the main criterion. In the case of successfully aligned series, a dense point cloud was produced, which was also subjected to analysis. Based on these results, appropriate procedures for photogrammetric processing were determined when conditions that may negatively affect image quality are known in advance.

KEYWORDS

Photogrammetry, Image quality, Alignment, Dense point cloud

INTRODUCTION

Photogrammetry has nowadays established itself in many scientific fields, where it is increasingly used, e.g., for documentation of historical monuments [1, 2], its use in combination with various types of UAVs [3] for capturing the Earth's surface is very widespread, its use in landscape monitoring for natural hazards is no less frequent [4, 5], but it can also be used in healthcare [6].

Nowadays, with the development of technology, the possibilities by which photogrammetric data can be acquired are expanding and the range of tools that can improve the quality of the resulting photogrammetric model and improve its accuracy is widening.

The different uses and processing conditions in the case of photogrammetry also differ in the data acquisition strategy. The use of terrestrial photogrammetry is common [7, 8, 9], while nowadays

photogrammetry using UAVs [10, 11, 12] or a combination of both methods is gaining prominence. Another option is to combine photogrammetry with LiDAR (Light Detection And Ranging) technology [13, 14] or to combine the resulting product with laser scanning output [15] or satellite imagery [16]. It is now common practice to use UAVs with a built-in GNSS receiver [17], which helps to georeference the resulting model more efficiently, while different methods of receiver position processing can be used [5, 18]. Although georeferencing using GCPs (ground control points) is still common today [10, 19], paths to direct georeferencing without the use of GCPs are being developed [20, 21].

However, the wide range of applications of this technology also entails different conditions under which photogrammetric documentation takes place. These conditions can affect the quality of the images, which are then used as an input into the processing. A photogrammetric model can only be produced from images that capture the same scene. The quality of the images is therefore crucial for successful processing, as reduced image quality (e. g. because of blurring) means degraded conditions for the alignment of the images due to their ambiguity.

Each of the photogrammetric software has a different computational kernel, so the same series of images will be produced differently in different software.

The quality of the images can be calculated in different ways [22], some photogrammetric software already has this function directly integrated [23], and this technology will be used later in this paper.

This paper aims to experimentally analyse the sensitivity to reduced quality of input images and the ability to process these images for three selected software. A total of 24 image series capturing six different surfaces are used for this purpose - each surface is imaged in four series with different image quality. The quality of the images is assessed using a coefficient that is generated in Agisoft Metashape Professional software.

The aspects monitored are in particular the ability of each software to process the reduced quality images and the quality of this processing. From these results, conclusions are then drawn regarding the suitability of the use of each software for processing degraded images and, in particular, recommendations for imaging under previously known degraded imaging conditions that may have a negative impact on image quality.

MATHERIALS AND METHODS

This chapter will describe the instruments and software used for the experiment and specify the testing methodology and results.

Equipment and software

The processing was carried out using three different software as shown in Table 1.

Tab. 1 - Used software

Software	Version
Agisoft Metashape Professional	2.0.1
iTwin Capture Modeler	24.0.0
Pix4Dmapper	4.7.5

Imaging was performed with a Canon EOS 450D camera with Canon EF 40 mm f/2.8 STM lens, whose parameters are listed in Table 2.

Tab. 2 - Parameters of used camera

Parameter	Value
Focal length	40 mm
Sensor type	CMOS

Sensor size	22,3 x 14,9 mm
Image resolution	4272 x 2848 pix
Pixel size	5,21 x 5,21 μm

Workflow

The quality of the dense cloud is influenced by the number of tie points, i.e., the points used for the alignment of the individual images. In order to correctly assign positions to images relative to others, these points need to be correctly identified in the image, and this depends on the quality of the images. Using blurry images for processing negatively affects the ability of feature detection, thus negatively affects the count of tie points.

The image quality factor can be calculated in Agisoft Metashape Professional and is an indicator of the sharpness of the images [23], which is calculated as the ratio between the pixels of the original image and the image to which a Gaussian filter has been applied [24]. Factor acquires values from 0 to 1, higher factor implicates higher quality (sharpness) of the particular image. According to [23], it is recommended not to use images that have a quality factor lower than 0.5 for the calculation.

For the purpose of this paper, three different indoor surfaces, namely two types of wood (a slightly varnished cabinet and a table) and a carpet (Figures. 1-3), and three different outdoor surfaces, gravel, concrete and grass (Figures. 4-6), were selected and imaged with different quality, each in a total of four series.

Fig. 1 – Cabinet surface

Fig. 2 – Table surface

Fig. 3 – Carpet surface

Fig. 4 – Gravel surface

Fig. 5 – Concrete surface

Fig. 6 – Grass surface

The indoor shooting was done with as much light as possible entering the room, while the outdoor shooting was done in cloudy weather.

The aim of this experiment was to test the alignment for aerial topographic mapping, that is why the images were taken from a single distance of approximately 1.2 m from the surface, only nearly orthogonal to the surface, and although handheld, the imaging procedure simulated the flight of a drone during nadir imaging.

Six images were taken in the longitudinal direction (four in the case of the 'Table' series) and four images were taken in the lateral direction. To illustrate the imaging method, the camera positions for the Gravel 4 series are shown in Figure 7, including the number of overlapping images in each part of the cloud, Figure 8 shows diagram of images axes; the same configuration of camera

positions was followed for the other series. Thus, each image was taken with sufficient overlaps in

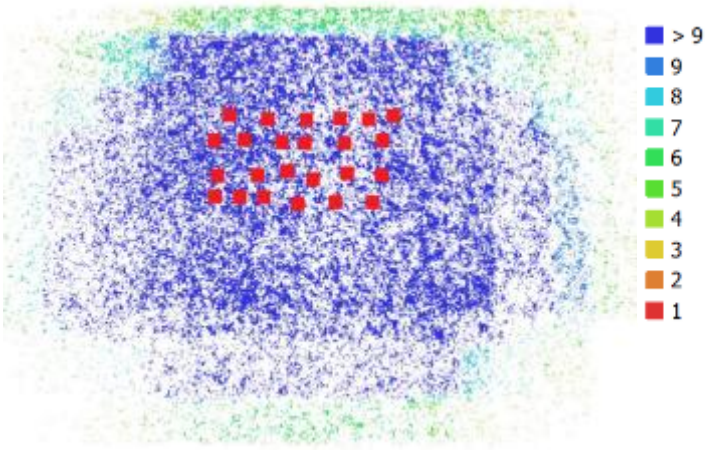

terms of processing the photogrammetric model.

Fig. 7 – Camera positions for the Gravel 4 series (red markers) and image overlap

Fig. 8 - Axes positions for the Gravel 4 series

First, the surfaces were photographed with the camera automatically set and in the highest possible quality, i.e., all images in the series had a quality factor greater than 0.5.

Then, two series were taken where the quality was artificially reduced. The camera was set to priority of time - in the case of one series the shutter was set to 1/25 s, in the case of the other to 1/8 s, ISO was set to 200 and aperture value was changing automatically in range of value f/2,8 - f/9 in case of interior series and f/2,8 - f/7 in case of exterior series. With these settings, the camera was moving when taking the picture. Finally, a series was taken where the quality was degraded only by manual blurring. The degradation of the images was always almost identical.

Series	Image count	Lowest quality factor	Highest quality factor	Average quality factor	Way of image degradation
Cabinet 1	24	0.55	0.83	0.75	
Cabinet 2	24	0.00	0.95	0.31	Exposure + movement
Cabinet 3	24	0.00	0.24	0.10	Exposure + movement
Cabinet 4	24	0.00	0.00	0.00	Blurring
Table 1	16	0.57	0.74	0.64	
Table 2	16	0.48	0.58	0.55	Exposure + movement
Table 3	16	0.00	1.00	0.43	Exposure + movement
Table 4	16	0.00	0.00	0.00	Blurring
Carpet 1	24	0.52	0.83	0.73	
Carpet 2	24	0.64	0.73	0.70	Exposure + movement
Carpet 3	24	0.54	0.73	0.63	Exposure + movement
Carpet 4	24	0.00	1.00	0.22	Blurring

All images were taken with autofocus on and lightning off.

The count of images of each series together with the extreme values of their quality factors are shown in Table 3 and Table 4, and Figures 9-14 show images with different quality of the selected surfaces.

Tab. 3 - Count of images and their quality factors for interior series

Tab. 4 - Count of images and their quality factors for exterior series

Series	Image count	Lowest quality factor	Highest quality factor	Average quality factor	Way of image degradation
Concrete 1	24	0.57	0.81	0.78	
Concrete 2	24	0.48	0.64	0.58	Exposure + movement
Concrete 3	24	0.37	0.70	0.60	Exposure + movement
Concrete 4	24	0.00	0.42	0.13	Blurring
Gravel 1	24	0.53	0.72	0.63	
Gravel 2	24	0.49	0.66	0.58	Exposure + movement
Gravel 3	24	0.44	0.70	0.50	Exposure + movement
Gravel 4	24	0.31	0.35	0.33	Blurring
Grass 1	24	0.67	0.82	0.76	
Grass 2	24	0.54	0.67	0.60	Exposure + movement
Grass 3	24	0.52	0.68	0.59	Exposure + movement
Grass 4	24	0.21	0.40	0.27	Blurring

Fig. 9 – Concrete - factor 0.23

Fig. 10 – Concrete - factor 0.58

Fig. 11 – Concrete - factor 0.80

Fig. 12 – Table - factor 0.00

Fig. 13 – Table - factor 0.53

Fig. 14 – Table - factor 0.73

All series were oriented in Agisoft Metashape Professional, iTwin Capture Modeler and Pix4Dmapper and in case of successfully oriented series (i.e., series where at least 2/3 of the images were oriented) a dense cloud was generated.

The alignment in Agisoft Metashape Professional was set to the Highest accuracy and there was no limit to the number of tie points per image to be generated. In the case of orientation in iTwin Capture Modeler, the number of tie points was set to High and in the case of orientation in Pix4Dmapper, the number of tie points was set to Automatic. There was no tie points filtering done after the alignment. Though Agisoft Metashape Professional offers function that filters tie points with low accuracy, which can increase the accuracy of following model / dense cloud, but the other two software do not include this function, so it was done in no software to achieve more comparable results.

Furthermore, if a dense point cloud was generated, it was generated with a quality of Ultra high in Agisoft Metashape Professional, sampling was set to 1 in iTwin Context Capture Modeler and in Pix4Dmapper the dense cloud was calculated from the original image resolution and with the point density set to High.

The subsequent comparison of the results examined the ability of the software to process each series and the quality of these processes, both visually and in terms of accuracy, where the main criterion was the quadratic mean of the reprojection error, i.e., the distance between the actual and the adjusted point position.

RESULTS

Tables 5 and 6 show the parameters of interior orientation for chosen series in all software, including optimized values for focal length in millimetres and distortion coefficients.

Figures 15 and 16 show distribution of tie points in two different series in all software. Figure 15 shows Grass 4 series (taken with manual blurring), where distribution of tie points through all software looks very similar, which happens in almost all series. On the other hand, Figure 16 shows one of two exceptions, where the distribution looks very different in different software and does not depict the shape of surface in Pix4Dmapper. These exceptions occur in case of Cabinet 1 (shown) and Grass 1, e. g. series taken with hight quality.

Tables 7 and 8 show the number of aligned images and the number of tie points from each series. In the case of successfully oriented series, the number of dense cloud points is also given.

Tab. 5 - Parameters of interior orientation for Cabinet series

Series	Parameter		Software		
			Agisoft Metashape Professional	iTwin Capture Modeler	Pix4Dmapper
Cabinet 1	Focal length [mm]		34,604	39,468	61,955
	Radial distortion coefficients	K1	-0,079	-0,095	-0,381
		K2	0,172	0,277	3,173
		K3	-0,035	-0,243	-8,111
	Tangential distortion coefficients	P1	0,000	-0,002	-0,010
		P2	0,003	0,002	0,001
Cabinet 2	Focal length [mm]		29,141	23,022	43,853
	Radial distortion coefficients	K1	-0,009	-0,003	0,068
		K2	-0,155	-0,076	-1,433
		K3	0,822	0,339	7,295
	Tangential distortion coefficients	P1	-0,009	0,020	-0,010
		P2	-0,005	0,027	0,013
Cabinet 3	Focal length [mm]		29,471	---	---
	Radial distortion coefficients	K1	-0,014	---	---
		K2	0,037	---	---
		K3	-0,265	---	---
	Tangential distortion coefficients	P1	0,020	---	---
		P2	-0,002	---	---
Cabinet 4	Focal length [mm]		65,679	25,036	42,048
	Radial distortion coefficients	K1	0,027	-0,042	0,013
		K2	-0,308	0,125	-1,122
		K3	1,359	-0,405	9,753
	Tangential distortion coefficients	P1	-0,031	-0,010	-0,002
		P2	0,033	0,011	0,006

Tab. 6 - Parameters of interior orientation for Concrete series

Series	Parameter		Software		
			Agisoft Metashape Professional	iTwin Capture Modeler	Pix4Dmapper
Concrete 1	Focal length [mm]		40,652	40,339	39,010
	Radial distortion coefficients	K1	-0,075	-0,077	-0,075
		K2	0,111	0,130	0,098
		K3	0,196	0,076	0,158
	Tangential distortion coefficients	P1	0,000	0,001	-0,004
		P2	0,001	0,000	0,001
Concrete 2	Focal length [mm]		68,240	58,543	40,912
	Radial distortion coefficients	K1	-0,179	0,052	-0,073
		K2	1,815	-0,620	0,808
		K3	-13,288	1,642	-5,636
	Tangential distortion coefficients	P1	0,009	-0,024	0,004
		P2	0,057	0,051	-0,004
Concrete 3	Focal length [mm]		39,631	28,212	38,753
	Radial distortion coefficients	K1	-0,027	-0,007	-0,015
		K2	0,041	-0,279	-0,361
		K3	0,019	1,028	2,824
	Tangential distortion coefficients	P1	-0,001	0,004	0,000
		P2	0,005	-0,020	0,001
Concrete 4	Focal length [mm]		41,446	31,069	---
	Radial distortion coefficients	K1	-0,074	-0,049	---
		K2	-0,292	-0,035	---
		K3	4,082	0,359	---
	Tangential distortion coefficients	P1	0,001	0,001	---
		P2	0,005	0,003	---

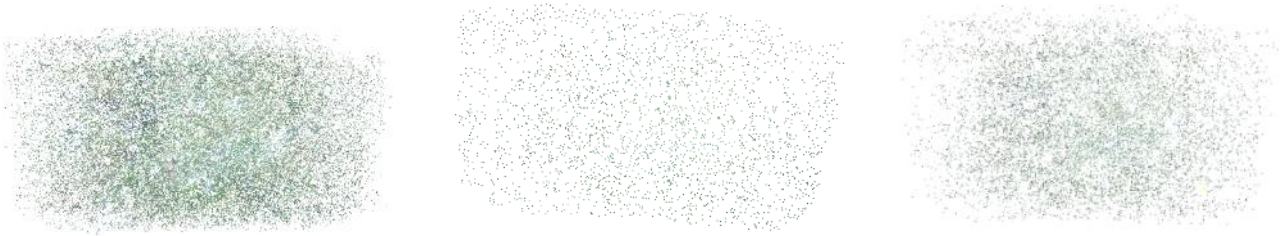

Fig. 15 - Tie points distribution for Grass 4 - top view - software (from the left) Agisoft Metashape Professional, iTwin Capture Modeler a Pix4DMapper

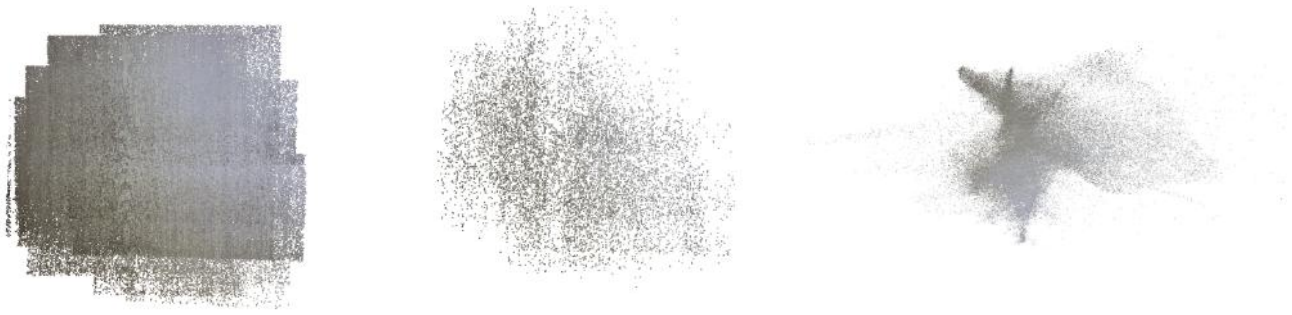

Fig. 16 - Tie points distribution for Cabinet 1 - top view - software (from the left) Agisoft Metashape Professional, iTwin Capture Modeler a Pix4DMapper

Tab. 7 - Counts of aligned images and points of sparse and dense clouds for interior series

		Agisoft Metashape Professional			iTwin Capture Modeler			Pix4Dmapper		
Series	Way of degradation	Images aligned	Tie points count	Dense cloud points count	Images aligned	Tie points count	Dense cloud points count	Images aligned	Tie points count	Dense cloud points count
Cabinet 1		24/24	296 343	37 916 525	24/24	10 788	33 192 366	24/24	281 177	5 562 177
Cabinet 2	time, moving	24/24	18 342	10 602 892	8/24	152	---	10/24	7 796	80 650
Cabinet 3	time, moving	5/24	540		0/24	---	---	0/24	---	---
Cabinet 4	blurring	24/24	8 157	5 721	24/24	142	1 617 774	24/24	3 424	---
Table 1		16/16	135 620	21 903 710	16/16	5 255	22 055 999	16/16	138 511	36 427
Table 2	time, moving	5/16	701		0/16	---	---	0/16	---	---
Table 3	time, moving	2/16	13		0/16	---	---	0/16	---	---
Table 4	blurring	16/16	2 686	1 303	16/16	165	3 507 995	0/16	---	--
Carpet 1		24/24	588 601	31 583 814	24/24	17 792	25 749 335	24/24	304 902	12 666
Carpet 2	time, moving	2/24	15		0/24	---	---	0/24	---	---
Carpet 3	time, moving	23/24	59 133	16 461 716	20/24	1 415	7 933 943	18/24	60 421	5 109
Carpet 4	blurring	24/24	6 838	58 859	24/24	592	22 235 142	18/24	2 816	---

Tab. 8 - Counts of aligned images and points of sparse and dense clouds for exterior series

		Agisoft Metashape Professional			iTwin Capture Modeler			Pix4Dmapper		
Series	Way of degradation	Images aligned	Tie points count	Dense cloud points count	Images aligned	Tie points count	Dense cloud points count	Images aligned	Tie points count	Dense cloud points count
Concrete 1		24/24	835 420	23 800 971	24/24	15 271	20 282 290	24/24	164 805	---
Concrete 2	time, moving	15/24	6 321	---	8/24	625	---	9/24	4 752	---
Concrete 3	time, moving	24/24	64 934	17 385 536	20/24	1 600	22 493 185	20/24	24 690	2 753
Concrete 4	blurring	24/24	10 985	888 389	24/24	844	21 577 319	0/24	---	---
Gravel 1		24/24	587 177	43 860 040	24/24	20 194	33 490 022	24/24	289 441	14 041 698
Gravel 2	time, moving	11/24	11 505	---	8/24	104	---	0/24	---	---
Gravel 3	time, moving	22/24	75 646	24 568 448	20/24	1 530	---	19/24	108 026	12 770
Gravel 4	blurring	24/24	67 044	8 691 866	24/24	6 946	21 135 779	24/24	61 524	---
Grass 1		24/24	675 243	23 822 714	24/24	11 406	45 103 792	24/24	200 509	950
Grass 2	time, moving	21/24	6 861	2 014 327	20/24	380	---	0/24	---	---
Grass 3	time, moving	14/24	21 574	---	15/24	540	---	11/24	26 006	2 359
Grass 4	blurring	24/24	35 961	44 873 542	24/24	2 725	22 150 156	24/24	36 590	---

From Tables 7 and 8, it can be seen that with the exception of the Grass 3 series, Agisoft Metashape Professional was able to orient more images than the other two software. Regarding the number of tie points, in four cases Pix4Dmapper software generated the highest number of points, but in the remaining cases Agisoft Metashape Professional again generated the highest number. In the case where a dense cloud was produced by both Agisoft Metashape Professional and iTwin Capture Modeler, Agisoft Metashape Professional generated the higher number of dense cloud points in six cases, iTwin Capture Modeler in eight cases. Pix4Dmapper generated very sparse clouds in all cases or did not generate them at all despite successful orientation. This also occurred in three cases in iTwin Capture Modeler.

The reprojection errors for each series are shown in Tables 9 and 10 below. At first glance, it can be seen that the error values generated by Pix4Dmapper are significantly lower than those of the remaining software. The series that were photographed with high accuracy (marked as 1) show very similar error values for the other two software, while the other series, with one exception, show smaller errors for iTwin Capture Modeler, in some cases very significantly.

Tab. 9 - RMS of reprojection errors for interior series

Series	RMS of reprojection error [pix]		
	Agisoft Metashape Professional	iTwin Capture Modeler	Pix4Dmapper
Cabinet 1	0.83	0.70	0.33
Cabinet 2	2.28	1.11	0.28
Cabinet 3	1.84	---	---
Cabinet 4	4.51	1.42	0.23
Table 1	0.85	0.66	0.20
Table 2	2.31	---	---
Table 3	1.24	---	---
Table 4	3.58	1.59	---
Carpet 1	0.53	0.51	0.16
Carpet 2	1.35	---	---
Carpet 3	1.37	1.10	0.20
Carpet 4	3.04	1.48	0.20

Tab. 10 - RMS of reprojection errors for exterior series

Series	RMS of reprojection error [pix]		
	Agisoft Metashape Professional	iTwin Capture Modeler	Pix4Dmapper
Concrete 1	0.32	0.31	---
Concrete 2	1.86	1.40	0.18
Concrete 3	1.54	1.26	0.18
Concrete 4	2.12	0.97	---
Gravel	0.37	0.36	0.11
Gravel 2	1.52	1.25	---
Gravel 3	1.27	0.95	0.23
Gravel 4	1.44	0.93	0.23
Grass 1	0.50	0.55	0.30
Grass 2	2.14	2.31	---
Grass 3	1.92	1.40	0.27
Grass 4	2.04	1.28	0.29

In Figure 17 and Figure 18, dense clouds from the corresponding series are shown. They show that in the case of the lower quality series, the iTwin Capture Modeler produces the visually best clouds.

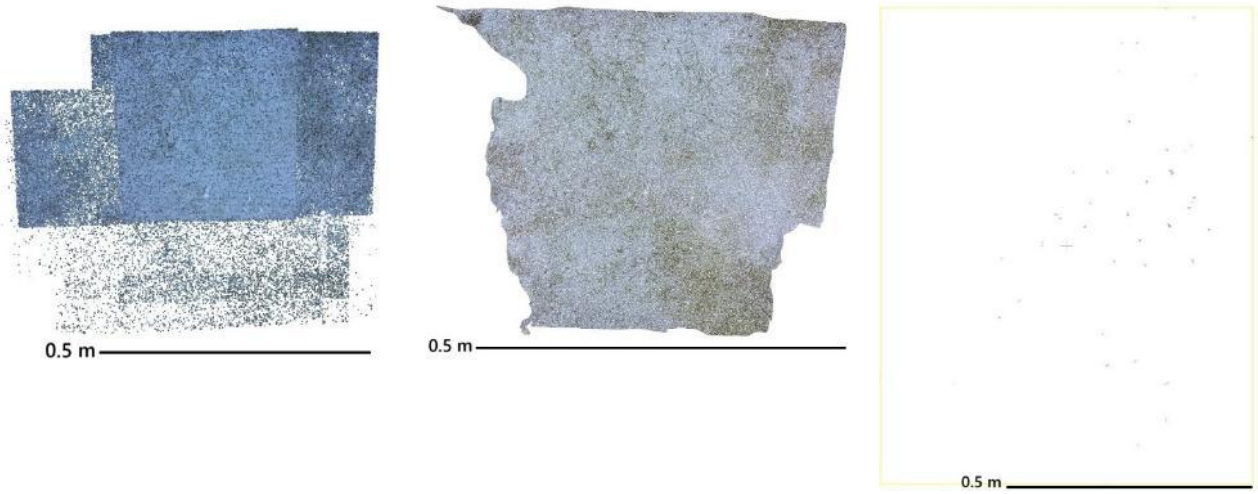

Fig. 17 – Dense cloud for Concrete 3 - software (from the left) Agisoft Metashape Professional, iTwin Capture Modeler a Pix4DMapper

Fig. 18 – Dense cloud for Gravel 1 - software (from the left) Agisoft Metashape Professional, iTwin Capture Modeler a Pix4DMapper

Some images, especially in case of the carpet, that stand out in the quality calculation are those that, although taken at reduced quality (Figure 19), were assessed as being of high quality. However, the orientation and calculation of the dense cloud are already consistent with the reduced quality. This is likely due to the nature of the surface, where the image after the application of the Gaussian filter is already very similar to the original image, so Agisoft Metashape is no longer able to distinguish that the original image is out of focus. However, the surface itself is already too difficult to process, and it is then of poor quality. Inverse case, image with quality calculated lower than 0.5 but in fact with high quality, did not appear in this experiment, but it does not mean, that it cannot happen. This implies that if it is requested to have absolute control over the image quality, it is necessary to do the manual check of all images.

Fig. 19 – Image of carpet with quality factor 0.94

From the reduced quality series all software produced a dense cloud that did not show the entire surface. If the poor conditions are known in advance, it is advisable to increase the number of images and extend the area imaged to ensure the entire area of interest is imaged more than necessary. According to the protocols, the reduced quality images in Agisoft Metashape Professional were usually processed in areas where there was an overlap of at least four images, in the case of iTwin Capture Modeler and Pix4Dmapper software at least three images, but in some cases five images were required for Agisoft Metashape Professional and iTwin Capture Modeler software. Examples of some of the required overlays are shown in Figures 20-22. For the high-quality series, locations with a required overlap of two images were processed in all software.

Despite requiring fewer overlapping images than Agisoft Metashape Professional and exhibiting by far the smallest reprojection errors, Pix4Dmapper was able to orient the fewest series and the resulting dense clouds were in most cases very sparse and thus unusable for further processing. Therefore, under poor conditions and this chosen imaging method, it is not advisable to use Pix4Dmapper for processing.

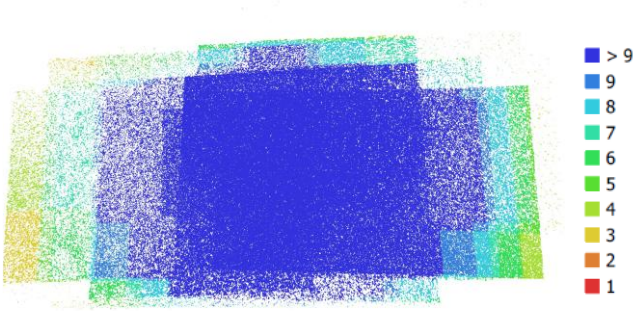

Fig. 20 – Images overlap on the produced parts of the dense cloud from the Gravel 3 series in Agisoft Metashape Professional

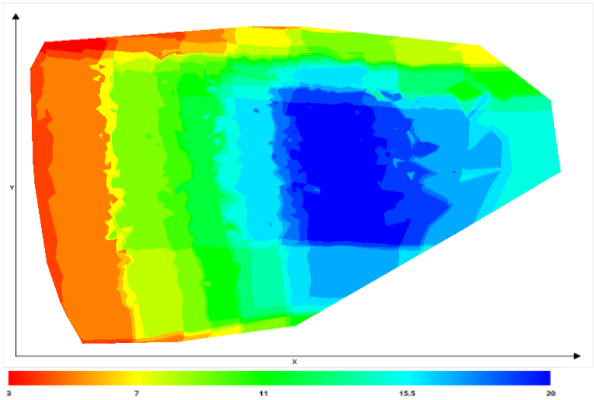

Fig. 21 – Images overlap on the produced parts of the dense cloud from the Gravel 3 series in iTwin Capture Modeler

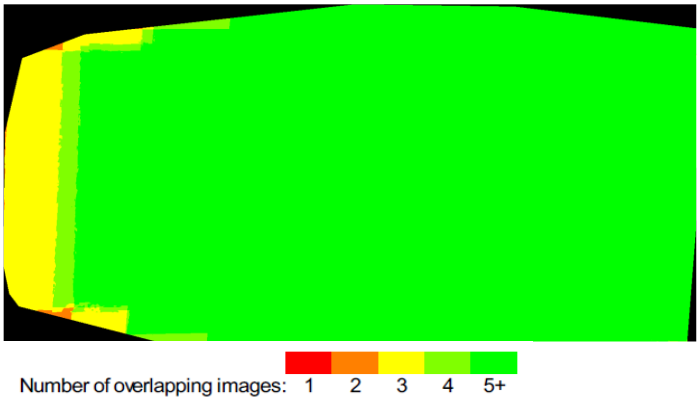

Fig. 22 – Images overlap on the produced parts of the dense cloud from the Gravel 3 series in Pix4Dmapper

CONCLUSION

As base of the testing, six different surfaces were captured with different image quality (4 series with different quality degradation), these series of images were then processed in Agisoft Metashape Professional, iTwin Capture Modeler and Pix4Dmapper. In terms of exterior orientation and number of tie points, Agisoft Metashape Professional performs the best, being able to orient even lower quality images and generate significantly higher numbers of tie points than iTwin Capture Modeler, however, it requires more image overlap than the other two software. iTwin Capture Modeler, on the other hand, produces the highest visual quality dense clouds of all the software tested. Pix4Dmapper has the lowest reprojection errors but oriented the fewest series and most of the dense clouds produced by it were unusable for further processing.

The analysis suggests that if the poor imaging conditions are known in advance, more images should be taken, so that the area of interest is always present in at least three or four images overlapping, depending on the software in which the further processing takes place, instead of the required two. Basically, using two images to create a model allows no control and the quality of alignment then depends on the image quality. When the quality is low, there is no control possible and in extreme cases it makes the alignment impossible. Required count of low-quality images to process the alignment then depends on the algorithms and abilities of particular software.

Thus, if the accuracy requirements do not need to be met, the reduced quality of the input images need not be an obstacle if the more stringent imaging conditions are met. Otherwise, although the software is able to orient the images in some cases, the reprojection error already

shows higher values. Therefore, it is advisable to follow the recommended quality factor limit of at least 0.5 and in case of a peculiar surface, the user should check the quality of the images themselves, as even a high-quality factor may not guarantee a good image.

ACKNOWLEDGEMENTS

This research was funded by the Grant Agency of CTU in Prague – grant number SGS24/047/OHK1/1T/11

REFERENCES

[1] Matoušková, E.; Pavelka, K.; Smolík, T. and Pavelka, K. Earthen Jewish Architecture of Southern Morocco: Documentation of Unfired Brick Synagogues and Mellahs in the Drâa-Tafilalet Region. Online. Applied Sciences. 2021, roč. 11, č. 4. ISSN 2076-3417. Dostupné z: https://doi.org/10.3390/app11041712. [cit. 2025-01-07].

[2] Šedina, J.; Hůlková, M.; Pavelka, K. and Pavelka, Jr, K. RPAS for documentation of Nazca aqueducts. Online. European Journal of Remote Sensing. 2019, roč. 52, č. sup1, s. 174-181. ISSN 2279-7254. Dostupné z: https://doi.org/10.1080/22797254.2018.1537684. [cit. 2025-01-09].

[3] Jon, J.; Koska, B. and Pospíšil, J. (2013) Autonomous Airship Equipped by Multi-sensor Mapping Platform, The International Archives of the Photogrammetry, Remote Sensing and Spatial Information Sciences, XL-5/W1, pp. 119-124. doi: 10.5194/isprsarchives-xl-5-w1-119-2013. [cit. 2025-01-09].

[4] Kovanič, Ľ.; Štroner, M.; Urban, R. and Blišťan, P. Methodology and Results of Staged UAS Photogrammetric Rockslide Monitoring in the Alpine Terrain in High Tatras, Slovakia, after the Hydrological Event in 2022. Online. Land. 2023, roč. 12, č. 5. ISSN 2073-445X. Dostupné z: https://doi.org/10.3390/land12050977. [cit. 2025-01-07].

[5] Žabota B. and Kobal, M. (2021) Accuracy Assessment of UAV-Photogrammetric-Derived Products Using PPK and GCPs in Challenging Terrains: In Search of Optimized Rockfall Mapping, Remote Sensing, 13(19), p. 3812. doi: 10.3390/rs13193812. [cit. 2025-01-07].

[6] Lim, Y. Ch.; Abdul Shakor, A. S. and Shaharudin, R. Reliability and Accuracy of 2D Photogrammetry: A Comparison With Direct Measurement. Online. Frontiers in Public Health. 2022, roč. 9. ISSN 2296-2565. Dostupné z: https://doi.org/10.3389/fpubh.2021.813058. [cit. 2025-01-07].

[7] Sánchez-García, E.; Balaguer-Beser, A.; Taborda, R. and Pardo-Pascual, J. E. Modelling Landscape Morphodynamics by Terrestrial Photogrammetry: An Application to Beach and Fluvial Systems. Online. ISPRS - International Archives of the Photogrammetry, Remote Sensing and Spatial Information Sciences. 2016, roč. XLI-B8, s. 1175-1182. ISSN 2194-9034. Dostupné z: https://doi.org/10.5194/isprsarchives-XLI-B8-1175-2016. [cit. 2025-01-09].

[8] Terrugi, L. B.; Rinaldi, M.; Chiaverini, I. and Ostuni, D. Application of Terrestrial Photogrammetry to the Measurement of a Riverbank Retreat. Online. ITALIAN JOURNAL OF ENGINEERING GEOLOGY AND ENVIRONMENT. 2011, s. 115-122. Dostupné z: https://doi.org/10.4408/IJEGE.2011-01.S-09. [cit. 2025-01-09].

[9] Nero, M. A.; Pinto Rocha, A.; Guerra Mamede, C.; Borba Schuler, C. A.; Da Costa Temba, P. et al. Positional accuracy in close-range photogrammetry through Topography and Geodesy. Online. Revista de Arquitectura. 2023, roč. 25, č. 2. ISSN 2357-626X. Dostupné z: https://doi.org/10.14718/RevArq.2023.25.3659. [cit. 2025-01-09].

[10] Chen, X.; Pan, S. and Chen, G. 3D model construction and accuracy analysis based on UAV tilt photogrammetry. Online. IOP Conference Series: Earth and Environmental Science. 2022, roč. 1087, č. 1. ISSN 1755-1307. Dostupné z: https://doi.org/10.1088/1755-1315/1087/1/012047. [cit. 2025-01-09].

[11] Vacca, G.; Dessì, A. and Sacco, A. (2017) The Use of Nadir and Oblique UAV Images for Building Knowledge, ISPRS International Journal of Geo-Information, 6(12), p. 393. doi: 10.3390/ijgi6120393. [cit. 2025-01-07].

[12] Blistan, P.; Kovanič, Ľ.; Zelizňaková, V. and Palková, J. Using UAV photogrammetry to document rock outcrops. Online. Acta Montanistica Slovaca. Roč. 21, č. 2, s. 154-161. Dostupné z: https://www.researchgate.net/profile/Peter-Blistan/publication/305781724_Using_UAV_photogrammetry_to_document_rock_outcrops/links/57a1b40408aeb16048331a5a/Using-UAV-photogrammetry-to-document-rock-outcrops.pdf. [cit. 2025-01-09].

[13] Štroner, M.; Urban, R.; Křemen, T.; Braun, J. UAV DTM Acquisition in a Forested Area—Comparison of Low-Cost Photogrammetry (DJI Zenmuse P1) and LiDAR Solutions (DJI Zenmuse L1). Eur. J. Remote Sens. 2023, 56, 2179942. [cit. 2025-01-07].

[14] Fuad, N. A., Ismail, Z., Majid, Z., Darwin, N., Ariff, M. F. M., Idris, K. M., a Yusoff, A. R. (2018, July 31). Accuracy evaluation of digital terrain model based on different flying altitudes and conditional of terrain using UAV LiDAR technology. IOP Conference Series: Earth and Environmental Science, 169, 012100. https://doi.org/10.1088/1755-1315/169/1/012100. [cit. 2025-01-07].
[15] Majid, Z.; Ariff, M. F. M.; Idris, K. M.; Yusoff, A. R.; Idris, K. M. et al. Three-Dimensional Mapping of an Ancient Cave Paintings Using Close-Range Photogrammetry and Terrestrial Laser Scanning Technologies. Online. The International Archives of the Photogrammetry, Remote Sensing and Spatial Information Sciences. 2017, roč. XLII-2/W3, s. 453-457. ISSN 2194-9034. Dostupné z: https://doi.org/10.5194/isprs-archives-XLII-2-W3-453-2017. [cit. 2025-01-09].
[16] Chen, Ch.; Tian, B.; Wu, W.; Duan, Y.; Zhou, Y. et al. UAV Photogrammetry in Intertidal Mudflats: Accuracy, Efficiency, and Potential for Integration with Satellite Imagery. Online. Remote Sensing. 2023, roč. 15, č. 7. ISSN 2072-4292. Dostupné z: https://doi.org/10.3390/rs15071814. [cit. 2025-01-09].
[17] Forlani, G., Dall'asta, E., Diotri, F., Cella, U. M. D., Roncella R., and Santise, M. (2018, February 17). Quality Assessment of DSMs Produced from UAV Flights Georeferenced with On-Board RTK Positioning. Remote Sensing, 10(2), 311. https://doi.org/10.3390/rs10020311. [cit. 2025-01-07].
[18] Dinkov, D. Accuracy assessment of high-resolution terrain data produced from UAV images georeferenced with on-board PPK positioning. Online. Journal of the Bulgarian Geographical Society. 2023, roč. 48, s. 43-53. ISSN 2738-8115. Dostupné z: https://doi.org/10.3897/jbgs.e89878. [cit. 2025-01-09].
[19] Güngör, R.; Uzar, M.; Atak, B.; Yilmaz, O. S. and Gümüş, E. Orthophoto production and accuracy analysis with UAV photogrammetry. Online. Mersin Photogrammetry Journal. 2022, roč. 4, č. 1, s. 1-6. ISSN 2687-654X. Dostupné z: https://doi.org/10.53093/mephoj.1122615. [cit. 2025-01-09].
[20] Teppati Losè, L.; Chiabrando, F. and Giulio Tonolo, F. (2020) Boosting the Timeliness of UAV Large Scale Mapping. Direct Georeferencing Approaches: Operational Strategies and Best Practices, ISPRS International Journal of Geo-Information, 9(10), p. 578. doi: 10.3390/ijgi9100578. [cit. 2025-01-07].
[21] Štroner, M., Urban, R., Seidl, J., Reindl, T., and Brouček, J. (2021, March 31). Photogrammetry Using UAV-Mounted GNSS RTK: Georeferencing Strategies without GCPs. Remote Sensing, 13(7), 1336. https://doi.org/10.3390/rs13071336. [cit. 2025-01-07].
[22] Matuzevičius, D.; Urbanavičius, V.; Miniotas, D.; Mikučionis, Š.; Laptik, R. et al. Key-Point-Descriptor-Based Image Quality Evaluation in Photogrammetry Workflows. Online. Electronics. 2024, roč. 13, č. 11. ISSN 2079-9292. Dostupné z: https://doi.org/10.3390/electronics13112112. [cit. 2025-01-09].
[23] Online. In: Agisoft Metashape User Manual - Professional Edition, Version 2.0. Agisoft Metashape, s. 25. Dostupné z: https://www.agisoft.com/pdf/metashape-pro_2_0_en.pdf. [cit. 2024-07-13].
[24] Topic: What causes an Estimated Image Quality value >1? Online. Agisoft Metashape. Dostupné z: https://www.agisoft.com/forum/index.php?topic=9889.0. [cit. 2024-11-01].